A multi-step finite element approach for the prediction of the residual strength of impact damaged composite aerospace structures

E. Panettieri · D. Fanteria · A. Firrincieli

Abstract Long and expensive experimental campaigns required to develop aerospace composite structures could be significantly reduced if reliable numerical simulations were used to perform engineering studies of complex damaged structures. The numerical simulation of the response to impact and the evaluation of the residual strength of an impact damaged structure are achievable through a full simulation of the impact process. The resulting set of sequential analyses required to reproduce complex damage scenarios requires large computational resources. The possibility to perform accurate simulations of an impact damaged structure until failure (assessment of the residual strength of the structure) would constitute a major improvement. This could be achieved if one were able to initialize structural damage using results from previous impact simulations. A multi-step procedure is proposed which reconstructs the relevant damage scenario for a residual strength simulation performed within FE software ABAQUS. Damage is calculated by means of a UMAT routine that provides material constitutive behavior for ABAQUS 3D elements. The damage initialization or transfer between different simulations is obtained by means of dedicated external scripts that interact with the ABAQUS SDVINI routine. Firstly, the proposed procedure is assessed on simple plate test-cases with literature data, then on a stiffened panel incorporating typical complexities of relevant aerospace structures.

Keywords Composites impact damage · composite structures residual strength · Damage simulation · Finite Element

E. Panettieri
University of Pisa, Department of Civil and Industrial Engineering - Aerospace division, via G. Caruso 8, 56122 Pisa, Italy
Tel.: +39-050-2217274
E-mail: enrico.panettieri@for.unipi.it

D. Fanteria
University of Pisa, Department of Civil and Industrial Engineering - Aerospace division, via G. Caruso 8, 56122 Pisa, Italy
Tel.: +39-050-2217266
E-mail: daniele.fanteria@unipi.it

A. Firrincieli
University of Pisa, Department of Civil and Industrial Engineering - Aerospace division, via G. Caruso 8, 56122 Pisa, Italy

1 Introduction

The response to impacts and the residual strength of aerospace composite structures are typically evaluated through long, expensive experimental campaigns [1]. Experiments could be limited to model validation and to certification phases if reliable numerical simulations were smartly used to perform engineering studies of complex damaged structures [2].

Conventional FE simulations of an impact damaged structure follow a sequential approach and complex damage scenarios can be created by replicating multiple impact events through simulations. The resulting set of sequential analyses is time consuming and requires large computational resources.

The capability to perform accurate simulations of the behavior of an impact damaged structure until failure (with an assessment of the residual strength of the structure) would constitute a major step forward the design of better experiment to validate structural solutions and towards the reduction of the experimental effort to develop complex, damage tolerant, composite structures.

This result could be achieved if one were able to initialize structural damage using results from previous impact simulations.

A multi-step procedure is proposed which reconstructs a damage scenario for a complex structure by using results from previous analyses independently simulating impact events in different parts of the structure. Due to its nature the procedure is necessarily and profoundly linked to the FE software used to perform impact damage simulations. Due to previous experience [3,4], simulations for this work are performed within FE software ABAQUS, complemented with FORTRAN user-routines (UMAT) that reproduce the progressive damage of composite laminates [5]. The key idea is to use ABAQUS routine SDVINI to initialize damage variables. This can be accomplished if both intra- and inter-laminar damage are simulated via material user-routines, consequently a UMAT routine has to be developed which implements user defined traction-separation behavior for ABAQUS 3D cohesive elements.

Even though the proposed initialization technique can be used to initialize every State Damage Variable (SDV) defined in the UMAT routines, in this work the intra-laminar damage is momentarily deactivated to reduce computational effort for the larger simulations and only inter-laminar damage is reproduced.

By means of the proposed approach, different shapes of delaminated zones can be initialized:

– simple delamination shapes (i.e. circular or rectangular), defined analytically within the SDVINI routine and representative of artificial delaminations typically obtained in practice my means of teflon inserts between the plies;
– delaminations with arbitrary shapes reconstructed from Ultrasonic C-scanning images and loaded by the SDVINI from external files;
– inter-laminar damage transfer between different simulations which is obtained by means of two sets of dedicated external routines that interacts with the SDVINI. In this case, the first set extracts and stores damage data from results database files of the first analysis while the second one loads and reorganizes damage information and passes them to the SDVINI which initializes damage variables of the second analysis.

The proposed approaches for damage initialization are applied to different test cases, of increasing complexity, to assess their performances and provide a first verification.

The remainder of the paper is organized as follows. In the next section, the key aspects of the mixed-mode delamination model that is implemented in the UMAT are presented. Section 3 outlines the proposed approach for multi-step damage simulation and briefly presents specifics about the different operating modes to initialize damage depending on shape and source of the relevant information. Section 4 presents and discusses the results obtained by employing the proposed approach on three test-cases. The first two are simple plate test-cases for which literature data exist, then the capability of the proposed approach will be demonstrated on a stiffened panel. The last test-case incorporates typical complexities of relevant aerospace structures, but is still tractable with the complete sequential simulation whose results are used as a term of comparison. Finally, essential aspects of the proposed approach and the main results achieved are summarized in Sec. 5.

2 Inter-laminar damage modeling and simulation

Interlaminar damage phenomena in advanced composite materials may be modeled by defining cohesive interactions which can approximate the progressive creation of new fracture surfaces. According to the original formulation of Dugdale [6] and Barenblatt [7], a Cohesive zone Model hypnotizes a process (softening) zone located ahead of a crack tip where cohesive interactions, or tractions, are related to the interfacial separation, or displacement jump. The cohesive zone model can effectively capture the nucleation of new delamination fronts (onset) and the propagation of existing delaminations. A cohesive zone model can be combined with FE methods to develop interfacial cohesive elements which can placed between the composite material layers in standard FE analyses. Cohesive elements can simulate composite delamination processes very effectively. Such excellent performances are mainly due to the two key constituents of the cohesive zone model, upon which cohesive elements are based: the delamination surfaces kinematics, encompassing strong discontinuities in the displacement field, and the cohesive constitutive relationship which can model variable-mode loading at the delamination front. Due to their advantages, cohesive elements are currently available in major FE software packages, ABAQUS, for example, provides 2D and 3D cohesive elements offering various options for the constitutive laws to characterize the interlaminar behavior. Unfortunately user access to constitutive parameters is limited and damage initialization of standard cohesive elements is impossible. Consequently, we decided to exploit the possibility to couple an ABAQUS 3D, eight-nodes, cohesive element (COH3D8) with a user defined material routine (UMAT) which provides the cohesive constitutive relationship. This approach has two main
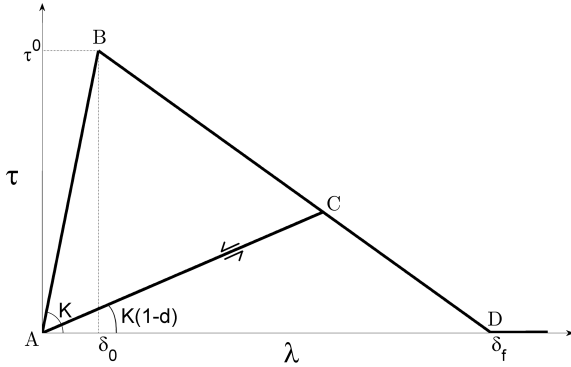
Fig. 1 Cohesive bi-linear constitutive law

advantages. The first one is that the FE software calculates the displacement discontinuities. The second one and most important one, is that damage variables used within the UMAT routine to define the cohesive constitutive behavior can be initialized according to the procedures that will be explained in the following sections. Cohesive element constitutive behavior is defined in terms of traction-separation relationships relating element nodal stresses to the relative displacement between corresponding pair of nodes[1].

Since the constitutive relationship requires an initial elastic range a bi-linear traction-separation law is the simplest possible constitutive model and one of the most used also because its parameters can be easily defined and identified. A bi-linear constitutive model, based on the assumptions presented in [8,9], has been implemented in the UMAT routine. The key features of the cohesive constitutive model are briefly presented in this section, further details can be found in [9]. The bilinear cohesive law is shown in figure 1, for a fixed mixed-mode ratio. The initial elastic response (curve AB) is defined by a penalty stiffness parameter: an high value of penalty stiffness is required to have a stiff connection between the element faces until traction reaches the interfacial strength of the material and damage initiates (Point B). The penalty stiffness and the interfacial strength define the displacement jump at the onset of damage (δ_0). If the displacement jump is increased beyond δ_0 the cohesive traction linearly decreases to zero (softening curve BD) and the initial stiffness is progressively decreased by the damage evolution law. When the displacement jump reaches a prescribed maximum value (point D), interface failure occurs and the interface load-bearing capacity vanishes. The area under the traction-separation curve represents the work needed to create a new delamination surface that is

the fracture toughness of the material at the considered mode-mixity. If at a given displacement jump (point C) the load is reversed the constitutive behavior is linear (curve CA) with a stiffness that is decreased according to the damage reached at point C.

Cohesive constitutive laws in ABAQUS relate the nominal stresses (nodal force components divided by the original area at each integration point) to the nominal strains (separations divided by the original thickness at each integration point, across the interface). Consequently the initial elastic constitutive relationship implemented in the UMAT routine is written as:

$$\boldsymbol{\tau} = \left\{ \tau_n \ \tau_s \ \tau_t \right\}^T = K \left\{ \varepsilon_n \ \varepsilon_s \ \varepsilon_t \right\}^T = K\boldsymbol{\varepsilon} \qquad (1)$$

where the strain component subscripts correspond to the three crack opening modes: opening (n), shearing (s) and tearing (t) mode. Nominal strains are computed according to their definition as $\varepsilon_\alpha = \delta_\alpha / T_0$ (with $\alpha = n, s, t$), where δ_n, δ_s and δ_t indicate the separation components and T_0 the original element thickness. Eventually, K indicates the value of the penalty stiffness that, after the damage is triggered, is progressively reduced by the increasing damage. The choice of the penalty stiffness value requires a trade-off between the necessity to have a stiff connection between adjoining elements (so that the initial elastic properties of the laminate are unaffected) and the opportunity to minimize numerical troubles (and the associated increases in the computational time): high values of penalty stiffness combined with the discontinuity of the tangent stiffness tensor at damage initiation can cause spurious traction oscillations [10]. In mixed mode conditions the traction-separation law is more conveniently expressed in terms of norms, that is:

$$\tau = \sqrt{\tau_n^2 + \tau_s^2 + \tau_t^2} = (\lambda - \delta_f) / \tau_0 (\delta_0 - \delta_f) \qquad (2)$$

$$\lambda = \sqrt{\langle \delta_n \rangle^2 + \delta_{shear}^2} \qquad \delta_{shear} = \sqrt{\delta_s^2 + \delta_t^2} \qquad (3)$$

where δ_0 and δ_f are the onset displacement jump and the failure displacement jump respectively. In the definition of λ MacAuley brackets[2] are used to neglect negative values of δ_n since contact between delaminated surfaces prevents compenetration. The mode-mixity in terms of displacement jump components is defined through parameter β:

$$\beta = \frac{\delta_{shear}}{\delta_n + \delta_{shear}} \qquad (4)$$

---

[1] Node pairs are defined so that a segment connecting the nodes in a pair is approximately normal to the fracture surface.

[2] Macauley brackets $\langle \cdot \rangle$ are defined so that: $\langle x \rangle = (x + |x|)/2$

For any value of the equivalent displacement jump λ a scalar damage variable d can be defined via the softening part of the traction-separation law. Damage d represent the effects of the interlaminar damage mechanisms which progressively reduce interface stiffness. The damage evolution law, for a given mixed-mode ratio (β), is defined as:

$$d = \frac{\delta_f \left(\lambda - \delta_0 \right)}{\lambda \left(\delta_f - \delta_0 \right)} \tag{5}$$

The damage variable increases only when the equivalent displacement jump λ at time t exceeds the maximum value reached by λ at any time $s \leq t$. When damage is active the constitutive relationship becomes:

$$\tau_\alpha = \left(1 - d \right) K \varepsilon_\alpha - dK\delta_{\alpha n} \left\langle -\varepsilon_\alpha \right\rangle \quad \alpha = n,\, s,\, t \tag{6}$$

where $\delta_{\alpha n}$ indicates the Kronecker delta. The linear traction-separation law at a given mode-mixity is identified through onset displacement jump δ_0 and failure displacement jump δ_f. These parameters can be expressed, through the mixed-mode ratio, in terms of pure modes quantities which can be more easily measured, or conveniently tuned, with standard tests. Damage onset is predicted by means of a quadratic criterion, with equal shearing and tearing strengths ($\tau_s^0 = \tau_t^0 = \tau_{shear}^0$):

$$\left(\frac{\left\langle \tau_n \right\rangle}{\tau_n^0} \right)^2 + \left(\frac{\tau_{shear}}{\tau_{shear}^0} \right)^2 = 1 \tag{7}$$

from which the onset displacement jump can be derived:

$$\begin{aligned} \delta_0 &= \delta_n^0 \delta_{shear}^0 \sqrt{\frac{\left(\frac{\beta}{1-\beta} \right)^2 + 1}{\left(\delta_{shear}^0 \right)^2 + \left(\frac{\beta}{1-\beta} \delta_n^0 \right)^2}} & \delta_n > 0 \\ \delta_0 &= \delta_{shear}^0 & \delta_n < 0 \end{aligned} \tag{8}$$

where δ_n^0 and δ_{shear}^0 and are the onset displacement jumps of pure modes. Interlaminar failure can occur at different mode-mixities and is assumed to occur when the energy release rate G reaches a critical value G^c. For any pure mode the critical energy release rates coincide with modal fracture toughness: G_n^c for the opening, G_s^c for the shearing and G_t^c for the tearing mode. Under mixed-mode loading the critical energy release rate is given as a function of pure modes fracture toughness and of the energy release rate components. Among the number of different expression that are available, the one proposed by Benzeggagh and Kenane (BK) in [11] will be used in this work under the assumption that $G_t^c = G_s^c$:

$$G_{eq}^c \left(B \right) = G_n^c + \left(G_s^c - G_n^c \right) \left(B \right)^\eta \tag{9}$$

where mode-mixity B is defined as:

$$B = \frac{G_{shear}}{G} \tag{10}$$

with $G_{shear} = G_s + G_t$ and $G = G_n + G_{shear}$. The values of toughness G_n^c and G_s^c and of mixed-mode interaction parameter η can be evaluated by means os standard tests such as Double Cantilever Beam (DCB) [12], End-Notched Flexure (ENF) and Mixed Mode Bending (MMB) [13].

The value of failure displacement jump δ_f is finally computed observing that, for a given mixed-mode ratio, the area under the traction-separation curve is the interlaminar critical fracture energy, thus:

$$\delta_f \left(B \right) = \frac{2 G^c \left(B \right)}{K \delta_0} \tag{11}$$

Then, by using the BK law the following relation is established for δ_f:

$$\delta_f \left(B \right) = \frac{\delta_n^0 \delta_n^f + \left(\delta_{shear}^0 \delta_{shear}^f - \delta_n^0 \delta_n^f \right) \left(B \right)^\eta}{\delta_0} \tag{12}$$

Since B is defined as a ratio of energy release rates for the current displacement jump, a relation can be established between B and β which reads:

$$B = \frac{G_{shear}}{G} = \frac{\beta^2}{1 - 2\beta + 2\beta^2} \tag{13}$$

3 The multi-step approach and its implementation

The proposed approach is based on the ABAQUS routine SDVINI which can be invoked by UMAT routines at runtime to define initial values of internal variables (STATEV). At the very beginning of an analysis (step 0) SDVINI is called for the integration points of each element to which an user-defined material is assigned, that is, for those elements whose constitutive behavior is defined via UMAT. ABAQUS passes to SDVINI information about coordinates of integration points and internal element IDs; both information are vital to define an initialization procedure for damage variables. Three different approaches to damage initalization are described in the following subsections.

3.1 Geometrical initialization

In this approach two distinct modes can be used to obtain an analytically defined domain where a damage variable (STATEV) is initialized to a prescribed value. In the simplest approach the domain is identified through geometrical coordinates within analytically defined boundaries; this requires the FE model be referred to a convenient coordinate system. A more efficient and flexible method to obtain analogous results consists in

creating, within ABAQUS, a set that includes all the elements in the domain to be initialized. Elements in such set share the same user-material and are initialized by the SDVINI. The drawback is that the UMAT is more complex since one must define multiple internal subroutines to characterize the constitutive behavior of different materials. The main advantage is that the graphic user interface (CAE) of the FE software can be advantageously used to define more general domains.

3.2 NDI-like initialization

In principle, the method which uses internal sets can initialize delaminations with arbitrary shapes reconstructed from Ultrasonic C-scanning (CSCAN) images but this can be extremely user-intensive and time consuming. A smarter approach, based on automatized image analysis, has been developed and it consists in the following key steps:

- the CSCAN images are acquired and transformed in binary black and white images to identify the delaminated areas;
- external dedicated scripts are used to gather the value of each pixel (0 for delaminated areas and 1 otherwise) and their normalized coordinates (one matrix for each inter-laminar layer);
- SDVINI reads the damage matrices and converts normalized coordinates into real ones to initalize damage variables in the UMAT routine.

3.3 Simulation-based initialization

This approach has been developed in order to recreate a complex damage scenario, within a large aerospace structure, avoiding the necessity to perform very long sequence of analysis steps to produce damage at each location of interest. As a first application in order to perform a preliminary assessment, a two-step procedure is used in this work. Two distinct FE simulations are performed: in the first one damage is produced in a FE model of a representative structure then damage is injected into a pristine model of the same structure. This application uses identical FE models for the analyses, at least locally, even though this limitation can be easily removed. The transfer of damage information between the two analyses is controlled by a procedure, based on two Python scripts, described as follows:

- a first Python script is used to access to the output database file (.odb), produced by the first analysis,

which stores the STATEV damage variables, internal element IDs [3] and integration point coordinates. The script save the relevant data into external text files for future use;
- the second Python script reads damage information from external text files and organizes them according to element IDs or integration point coordinates. The reordering of the damage information is carried out considering specific details [4] of the second FE analysis. The sorted data are vital to efficiently perform the initialization of the second analysis especially for large models;
- finally, SDVINI reads the sorted data and initialized the requested damage variables in the second analysis.

4 Results and discussion

In this section the results relevant to the following test-cases are presented:

1. a simple geometrical initialization of a circular artificial damage to simulate delamination-buckling under compression;
2. a NDI-like initialization test-case in which multiple measured delaminations are injected into a composite plate subjected to axial compression (in CAI-test like set-up);
3. a simulation-based initialization test-case where delaminations are produced in a stiffened panel via static indentation and then injected in a compression-buckling analysis that causes delamination growth.

### 4.1 Geometrical initialization test-case

The developed inter-laminar constitutive behavior, implemented in a dedicated UMAT routine, has been assessed by considering the Compression After Impact results of a carbon/epoxy specimen presented in [14] and reported in a dedicated example of Virtual Crack Closure Technique (VCCT) in [5]. This specific test-case has been chosen due to the following factors: a relatively simple defect within the laminate, i.e. circular delamination and a good set of experimental data in terms of force applied, deformation and propagation of delamination. Moreover the same test-case has been considered in [5] to evaluate the use of ABAQUS

---

[3] ABAQUS CAE assigns unique element IDs within a part instance, only at runtime unique element IDs are assigned within the whole model.

[4] In the current version the two models need to be identical in the areas interested by damage but can differs in terms of active part instances and boundary conditions.
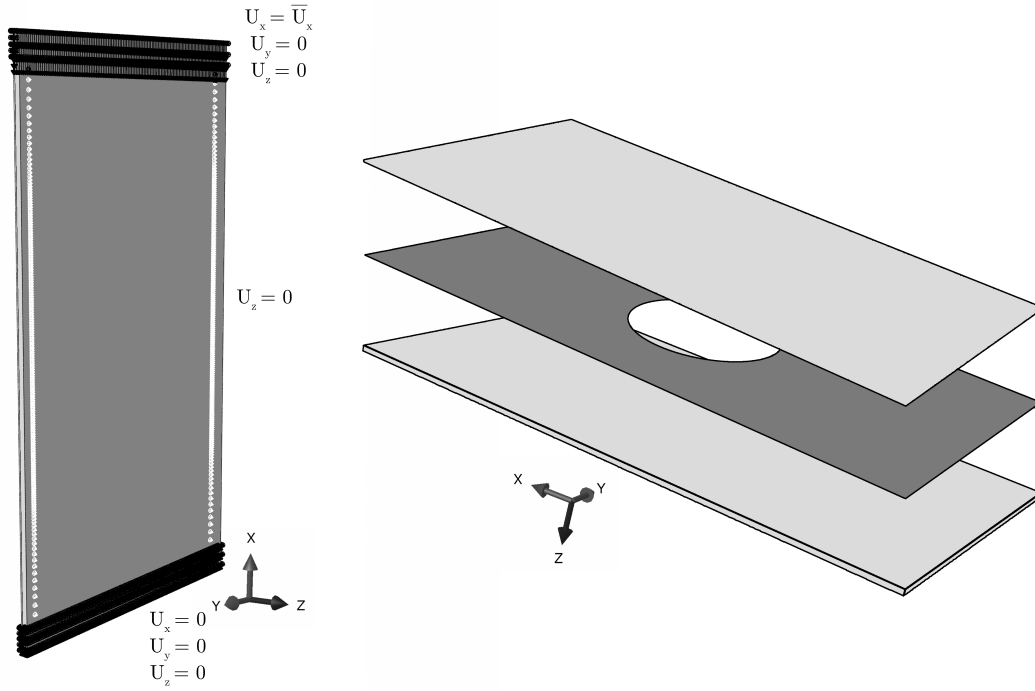
Fig. 2 Acquired (a) and intialized (b) delamination shapes
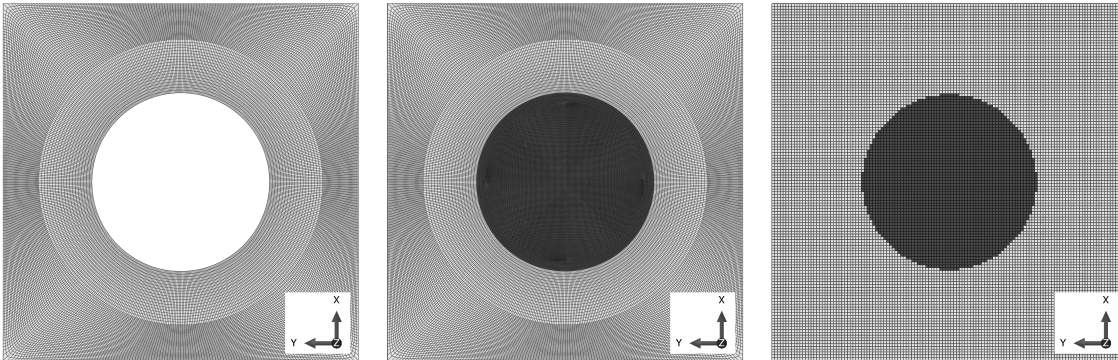
Fig. 3 FE models of the cohesive layer for the delamination buckling analyses: Hole UMAT (left), Radial UMAT (center) and Rectangular UMAT (right)

VCCT. The specimen has a $[(-45/+45/90/0)_2/-60/+60/-15/+15]_s$ lamination and is provided with a circular pre-existing delamination obtained inserting a teflon layer between the 5th and 6th ply $(-45/+45$ interface). Figure 2 shows the boundary conditions enforced in the Finite Element model together with an example of how the plate has been modeled: two sub-laminates with continuum shell elements $(SC8R)$ and one cohesive layer $(COH3D8)$. The two sub-laminates and the cohesive layer are linked with TIE constraints except for the model with the regular rectangular mesh. An imperfection, with the same shape of the first eigenvalue obtained with a previous linear buckle simulation, is provided with a maximum out-of-plane displacement of the thinnest sub-laminate equal to 0.1 mm. Three different version of the cohesive layer, shown in Figure 3, have been considered in order to compare different initialization strategies of the cohesive elements on the global solution. Axial strain are deduced from each simulation analogously to the experimental test in which strain gauges are placed in positions scarcely affected by the delamination or by the fixture (far field strain). More details can be found in [14]. Axial connectors with negligible stiffness have been used to simulate strain gauges
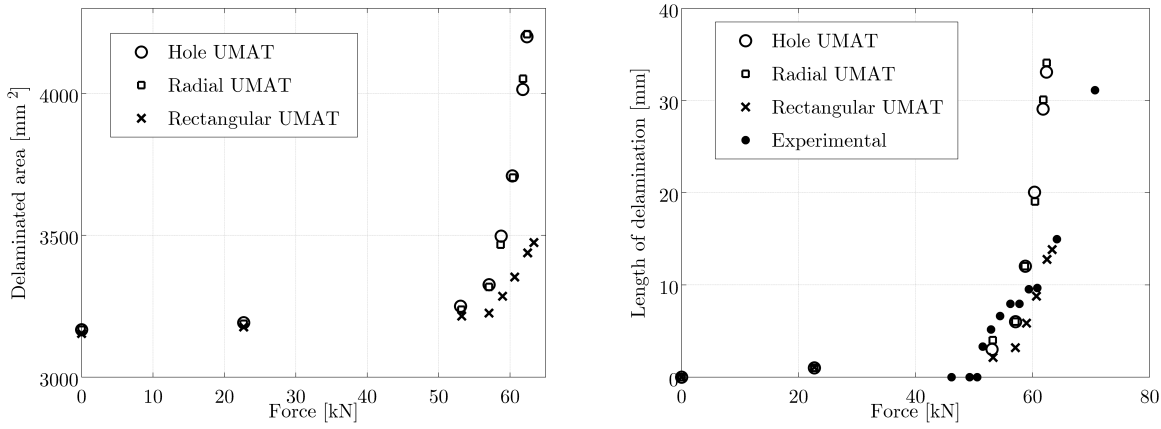
Fig. 5 Delaminated area vs. force (left) and delamination length vs. force (right)

readings. Figure 4 shows the applied force vs. the axial strain of the experimental test and the simulations. The numerical results well compares to the experimental ones and no appreciable differencies can be observed between the three modeling approaches. Analyses have been stopped in correspondence of the maximum damageable area (anulus around the hole in Figure 3). The
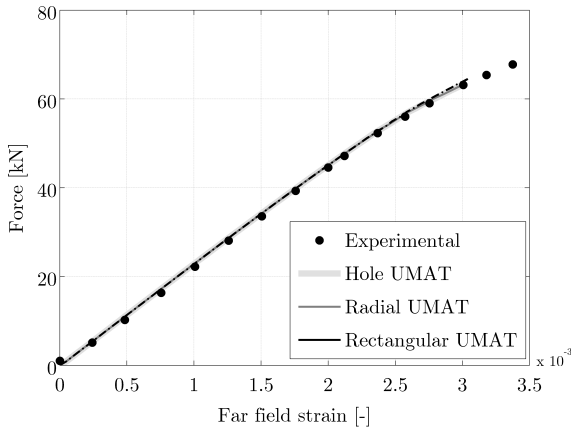

Fig. 4 Comparison of the force vs. far field strain between the experimental and numerical results

delaminated area of each simulation for fixed values of applied load is reported in Figure 5. In the same Figure a comparison between numerical and experimental data in terms of delamination length is also provided (length measured along the maximum propagation direction). The results of the model with initialized radial mesh (Radial UMAT) are identical to the one with the physical hole in the cohesive layer (Hole UMAT). Both models produces larger delaminations compared to the experimental data for loads above $60kN$. The model with the rectangular mesh produces smaller delaminated areas and thus delaminated length that are very close to the experimental data. These results highlight a remarkable sensitivity to the shearing mode fracture toughness and to the topology of the mesh which deserve further investigations. The results confirm that the geometrical initialization procedure is capable to correctly initialize inter-laminar damage and that the results of the initialized simulation (with the same damageable zone mesh) matches perfectly the one with the removed cohesive elements.

4.2 NDI-like initialization test-case

The method has been applied in a Compression After Impact (CAI) simulation for which experimental data of extension and position of delaminated areas are available [15]. The study reported the experimental results of impact and CAI tests on different materials and stacking sequences. Extension and position of the delaminations after each impact are also reported. In order to assess the proposed initialization procedure, we have chosen one delamination pattern in [15] to be used as input data. The specimen is 150 mm x 100 mm plate with a $[-45_4/45_4/0_3/90]_s$ lamination for a total thickness of 4.53 mm. This particular stacking sequence results in six delaminated interfaces placed between each group of equi-oriented plies. The Finite Element model

$U_x = \overline{U}_x$
$U_y = 0$
$U_z = 0$

$U_z = 0$

(a)

$U_x = 0$
$U_y = 0$
$U_z = 0$

(b)
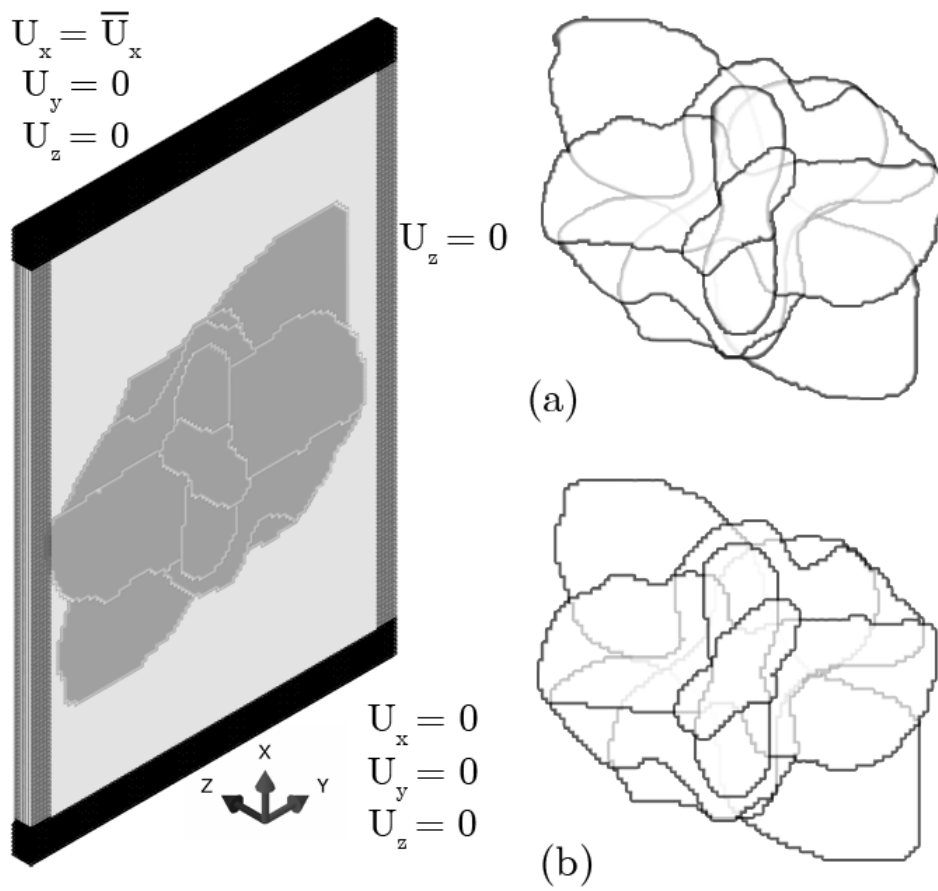
Fig. 6 Boundary conditions enforced to the model (left) and delamination shapes: original (a) and initialized (b)
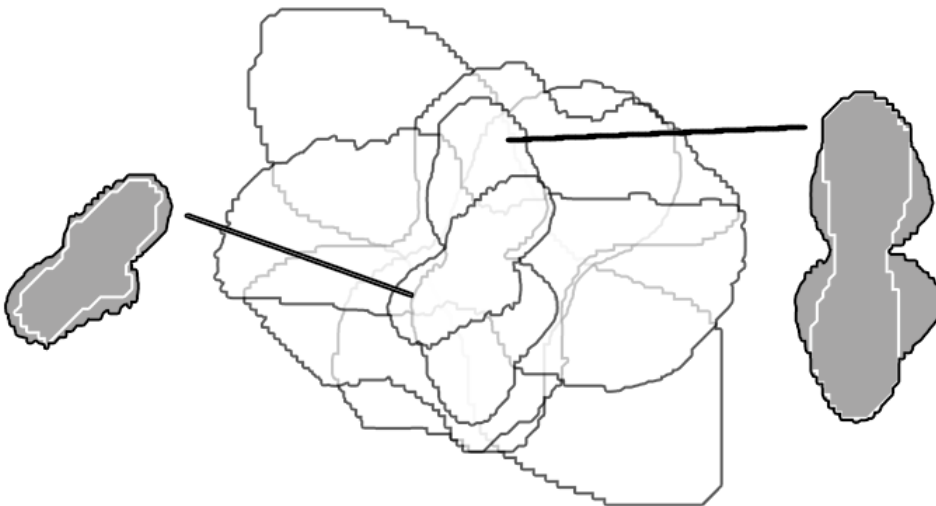
Fig. 7 Examples of the propagation of delaminated zones under compression load

is shown in Figure 6. The laminate has been reproduced by gathering together each group of plies in solid $C3D8$ elements spaced out by six inter-laminar layers of cohesive elements ($COH3D8$). Boundary conditions have been applied to reproduce the ones enforced by the CAI fixture. Figure 6 also shows the shapes of the delaminations captured from [15] (a) and the initialized ones (b), which present jagged edges due to the FE discretization. Figure 7 shows the evolution of delaminations at a given step time of the compression simulation. In the Figure the damaged zones (grey) of two cohesive layers are shown compared with initial delaminated shapes (thin white line). Even though the presented data have a qualitative purpose, this results show that the procedure is able to initalize multiple delaminations with realistic shapes and that the compression analysis produces delamination growth under load.

4.3 Simulation-based initialization test-case

As test-case to assess the simulation-based initialization procedure, an indentation simulation of a carbon/epoxy stiffened panel has been performed. The panel is $150 \times 250mm$ with a skin of $1mm$ thick and 2 stringers. The skin is a $[+45/-45/0/90]_s$ laminate modeled with two SC8R elements along the thickness. Thicker stringers (with a quasi-isotropic stacking sequence) are modeled in order to force a skin buckling behavior in order that the propagation of delaminations during the compression step be induced. Figure 8 shows the boundary conditions enforced to the model and other details of the FE model: the skin is partitioned so that an explicit ply-by-ply 3D model in correspondence of the indentor can reproduce delaminations and tied with the rest of the model; the indentor is placed in correspondence of one of the flange of the stringer (skin side) in order to produce both damage within the skin laminate and debonding between the skin and the stringer. The local laminate model has inter-laminar layers between each pair of ply and a cohesive layer which connects this portion of the skin with the flange of the stringer above in order to reproduce skin-stringer debonding.
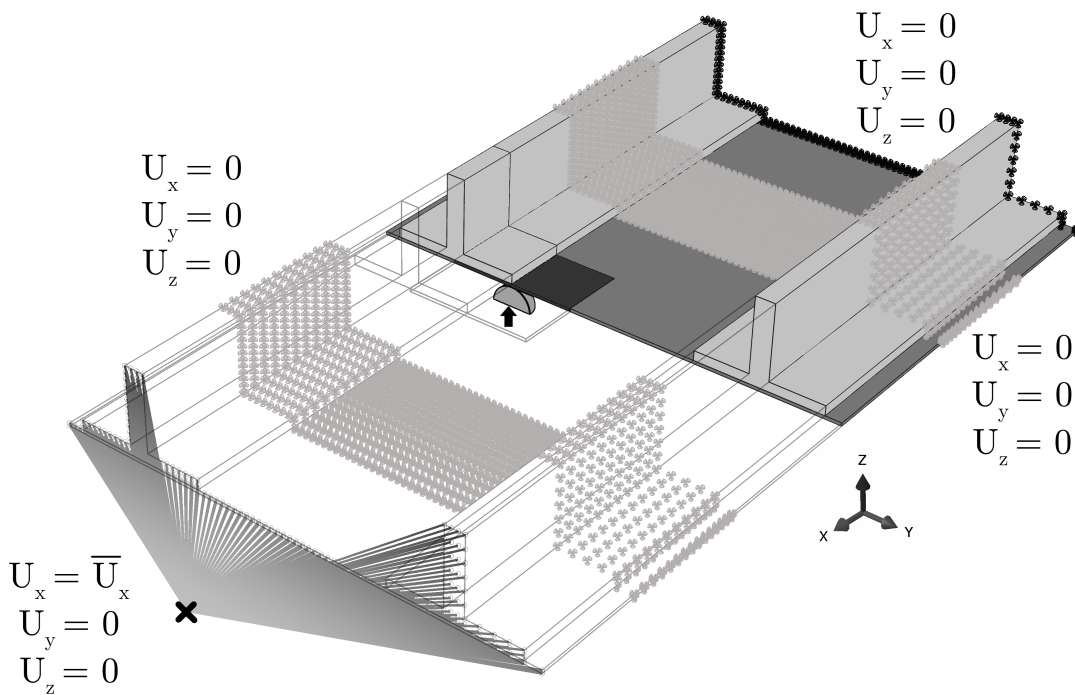
Two analyses are performed: the first is a three-steps sequential analysis in which the indentation step is followed by a step to damp residual vibrations and the final compression one, the second uses the damage obtained at the end of the first step (indentation step) of the sequential analysis to perform a stand-alone analysis of the panel compression. Figure 9 shows a flow-chart which summarizes the key points of both the sequential analysis (top in Figure 9) and the initialized one (bottom in Figure 9). Moreover, the damage data (delaminations), extracted from the sequential analysis and

transfered to the one to be initialized, are highlighted. Figure 10 shows the delaminated shapes at the end of the indentation step and at the end of the compression one of the sequential analysis. The results of the two analyses are compared in Figure 11 in terms of the out-of-plane displacement for a similar applied load and by reporting, in Figure 12, the computed delaminated areas of the two analyses at given loads. In Figure 12 the delaminated shape at the end of the compression step of the initialized analysis is also reported allowing a qualitative comparison with the identical one obtained in the sequential analysis.
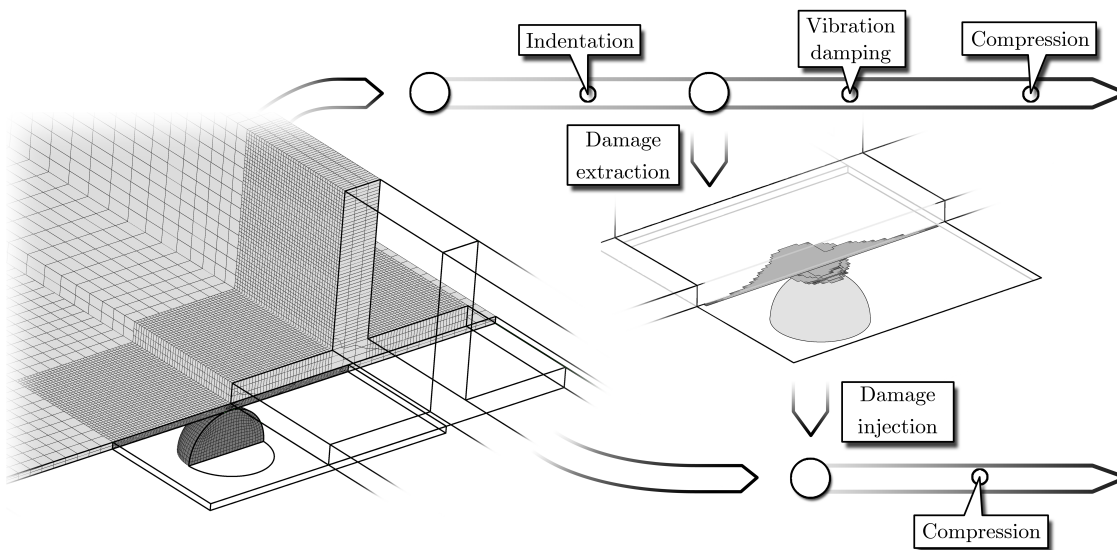
The obtained results show that the simulation-based initialization procedure is able to correctly initialize inter-laminar damage, extracted from a previous analysis, into a new model. Identical results in terms of both out-of-plane displacements and delaminated shapes are obtained by the two simulations, assessing, thus, the procedure.

5 Conclusions

Three different damage initialization techniques of increasing complexity have been developed and tested in dedicated test-cases obtaining promising results. In this work, inter-laminar damage has been considered, even though each of the technique can also handle intra-laminar damage. An UMAT routine has been developed and used to characterize the constitutive behavior of ABAQUS cohesive elements and to allow ABAQUS SDVINI routine be used to initialize damage. The geometric initialization technique can be easily used for analytically defined domains while, whether accurate NDI data are available, the NDI-like initialization technique is able to automatically inject the measured damaged areas in the FE model of interest. Eventually, the most complex of initialization techniques developed uses a combination of Python scripts to extract, organize and make available to the SDVINI the damage variables to be initialized. Each one of damage initialization techniques can be used to reproduce different damage scenarios on larger structures avoiding multiple sequential simulations. In particular, the simulation-based initialization technique can be used to store the results of complex damage events on a structure (such as impact events), in terms of damage variables and their location. Then, by initializing suitable larger structural model, the residual strength can be estimated for different damage scenarios.

$$U_x = 0$$
$$U_y = 0$$
$$U_z = 0$$

$$U_x = 0$$
$$U_y = 0$$
$$U_z = 0$$

$$U_x = 0$$
$$U_y = 0$$
$$U_z = 0$$

$$U_x = \overline{U}_x$$
$$U_y = 0$$
$$U_z = 0$$

Fig. 8 Enforced boundary conditions (different set of conditions are used for the different steps)

Indentation

Vibration damping

Compression

Damage extraction

Damage injection

Compression

Fig. 9 Flow-chart of the sequential analysis (top) and of the initialized one (bottom)

References

1. U.S. Department of Defense (2002) Composite materials handbook, vol. 1-4F. MIL-HDBK-17 rev F.
2. Davies G, Ankersen J (2008) Virtual testing of realistic aerospace composite structures. J Mater Sci 43:65866592. doi: 10.1007/s10853-008-2695-x
3. Longo G (2011) Models and methods to simulate low-energy impact damage on composite aerospace structures. Ph.D. Thesis, University of Pisa.
4. Fanteria D, Longo G, Panettieri E (2014) A non-linear shear damage model to reproduce permanent indentation caused by impacts in composite laminates. Compos. Struct. 111: 111-121.
5. Dassault Systemes Simulia Corp. (2014), Abaqus 6.13 User's Manual.
6. Dugdale DS (1960) Yielding of steel sheets containing slits. J Mech Phys Solids 8:100104
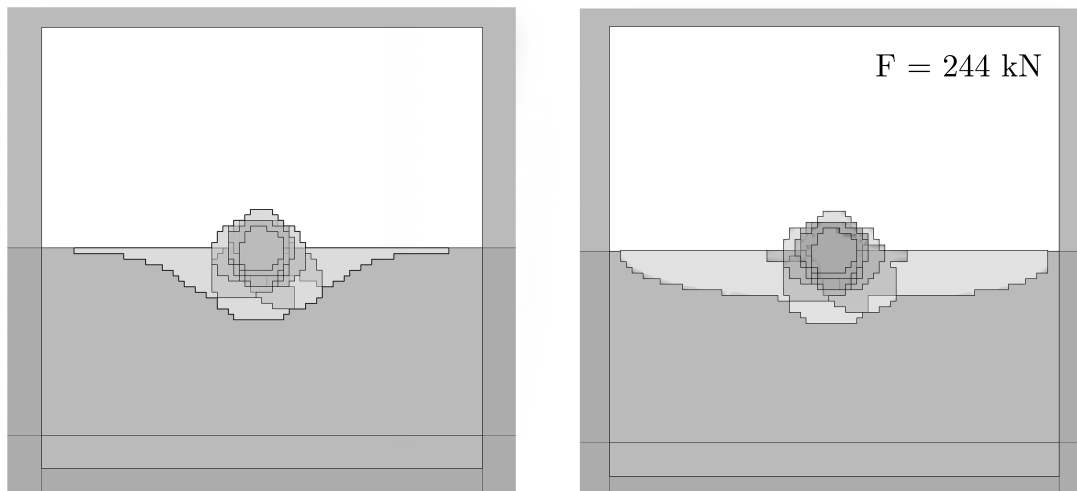
Fig. 10 Comparison of the delaminations pattern of the sequential analysis at the beginning and at the end of the compression step

F = 244 kN   F = 242 kN
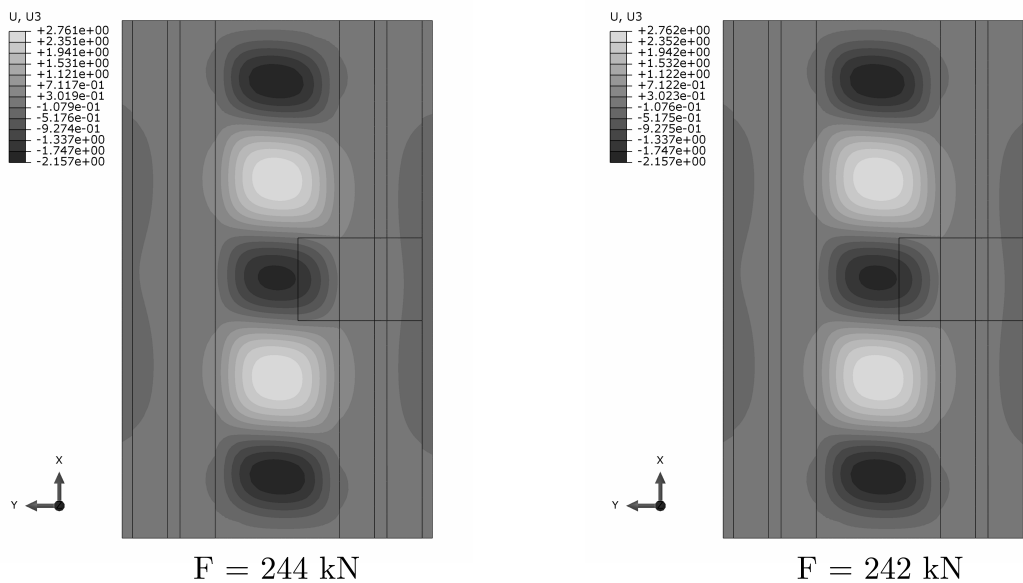
Fig. 11 Comparison of the out-of-plane (U3) displacement at the same time step of the sequential (left) and initialized analysis (right

7. Barenblatt G (1962) The mathematical theory of equilibrium cracks in brittle fracture. Adv Appl Mech 7:55129
8. Camanho PP, Davila CG, de Moura MF (2003) Numerical simulation of mixed-mode progressive delamination in composite materials. J Compos Mater 37:14151438. doi: 10.1177/002199803034505
9. Turon A, Camanho PP, Costa J, Dvila CG (2006) A damage model for the simulation of delamination in advanced composites under variable-mode loading. Mech Mater 38:10721089. doi: 10.1016/j.mechmat.2005.10.003
10. Schellekens JCJ, de Borst R (1992) On the numerical integration of interface elements. Int J Numer Methods Eng 36:4366.
11. Benzeggagh ML, Kenane M (1996) Measurement of mixed-mode delamination fracture toughness of unidirectional glass/epoxy composites with mixed-mode bending apparatus. Compos Sci Technol 49:43949
12. American Society for Testing and Materials Standard Test Method for Mode I Interlaminar Fracture Toughness of Unidirectional Fiber-Reinforced Polymer Matrix Composites. ASTM D5528-01.
13. American Society for Testing and Materials Standard Test Method for Mixed Mode I - Mode II Interlaminar Fracture Toughness of Unidirectional Fiber-Reinforced Polymer Matrix Composites. ASTM D6671/D6671M-06.
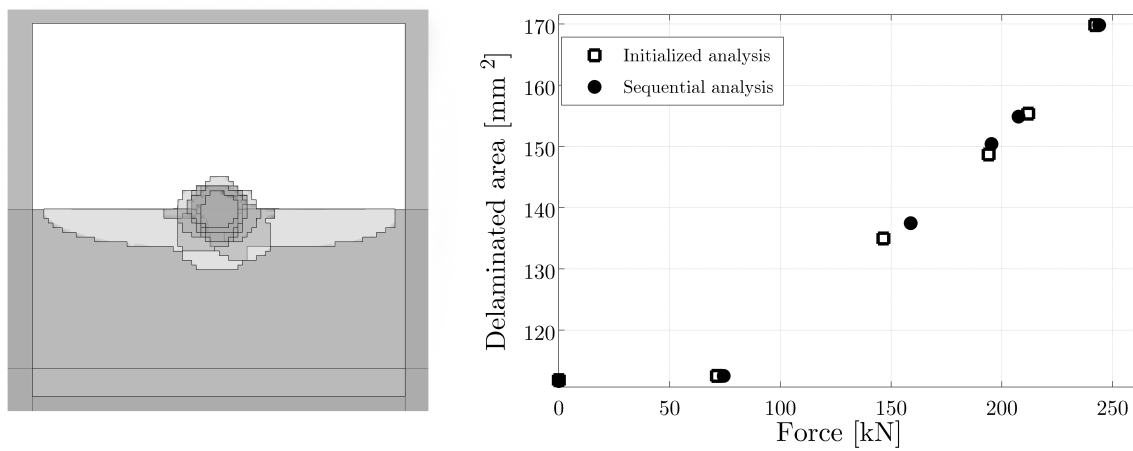
Fig. 12 Final configuration of the delaminations of the initialized analysis (left) and delaminated areas vs. applied force (right)

14. Reeder JR, Chunchu PB, Song K, Ambur DR (2002) Postbuckling and growth of delaminations in composite plates subjected to axial compression, 43rd AIAA/ASME/ASCE/AHS/ASC Structures, Structural Dynamics, and Materials Conference.
15. De Freitas M, Reis L (1998) Failure mechanisms on composite specimens subjected to compression after impact. Compos. Struct. 42:365-373.